

Estimates of fault strength from the Variscan foreland of the northern UK

Alex Copley^{1*} and Nigel Woodcock²

1: COMET, Bullard Labs, Department of Earth Sciences, University of Cambridge, Cambridge, UK

2: Department of Earth Sciences, University of Cambridge, Cambridge, UK

* Email: acc41@cam.ac.uk

₁ Abstract

₂ We provide new insights into the long-standing debate regarding fault strength,
₃ by studying structures active in the late Carboniferous in the foreland of
₄ the Variscan Mountain range in the northern UK. We describe a method
₅ to estimate the seismogenic thickness for ancient deformation zones, at the
₆ time they were active, based upon the geometry of fault-bounded extensional

7 basins. We then perform calculations to estimate the forces exerted between
8 mountain ranges and their adjacent lowlands in the presence of thermal and
9 compositional effects on the density. We combine these methods to calculate
10 an upper bound on the stresses that could be supported by faults in the
11 Variscan foreland before they began to slip. We find the faults had a low
12 effective coefficient of friction (i.e. 0.02–0.24), and that the reactivated pre-
13 existing faults were at least 30% weaker than unfaulted rock. These results
14 show structural inheritance to be important, and suggest that the faults had
15 a low intrinsic coefficient of friction, high pore-fluid pressures, or both.

16

17 Key words: Fault Strength, Variscan, Seismogenic thickness

18

19 **1 Introduction**

20 The rheology of active faults is a major source of debate. A general issue
21 concerns the magnitude of stresses that faults can support before breaking
22 in earthquakes, or undergoing creep at a significant rate. Previous studies
23 have used a range of techniques to address this question, and have obtained

24 a range of different results. The debate has often focused on estimating the
25 coefficient of friction of faults (either the intrinsic value, or the effective coef-
26 ficient of friction resulting from the combination of rock properties and pore
27 fluid pressures). Hydro-fracturing in boreholes has been used to infer that
28 the crust is cut by faults with an intrinsic coefficient of friction similar to that
29 suggested by ‘Byerlee’s Law’ (i.e. $\sim 0.6\text{--}0.8$; (Byerlee, 1978)), and hydrostatic
30 pore-fluid pressures (e.g. Brudy et al., 1997; Townend and Zoback, 2000). In
31 contrast, some experiments on fault rocks cored by boreholes have resulted
32 in much lower estimates of the intrinsic coefficient of friction (i.e. ≤ 0.3 ;
33 Lockner et al. (e.g. 2011); Ujiie et al. (e.g. 2013)). Geophysical arguments
34 have been made that imply similarly low effective coefficients of friction (e.g.
35 Lamb, 2006; Copley et al., 2011). The distribution of earthquake nodal plane
36 dips has been interpreted as evidence for both high intrinsic coefficients of
37 friction (e.g. ~ 0.6 ; Sibson and Xie (1998); Collettini and Sibson (2001)),
38 and also as an indicator of intrinsically low friction on fault planes [e.g. \leq
39 0.3 ; Middleton and Copley (2014); Craig et al. (2014)]. The resolution of
40 this debate has important implications for our understanding of lithosphere
41 rheology, and also for assessing earthquake hazard. If fault friction is low,
42 then earthquake stress-drops (commonly in the range of megapascals to tens

43 of megapascals (e.g. Kanamori and Anderson, 1975; Allmann and Shearer,
44 2009)) are likely to represent the majority of the pre-earthquake shear stress
45 on the fault plane, and significant time for stress build-up will be required
46 before earthquakes can nucleate again on a ruptured section of fault. If fault
47 friction is high, then stress-drops in earthquakes will be only partial, and
48 the timing of subsequent ruptures on a given fault could be highly variable.
49 In view of the uncertainty regarding fault friction, this study aims to pro-
50 vide new information by studying the late Carboniferous deformation in the
51 northern UK, in the foreland of the Variscan Mountain range. As part of
52 this work, we outline how to estimate the seismogenic thickness in ancient
53 deformation zones at the time they were active (by using a scaling between
54 seismogenic thickness and basin geometry), and describe a method to calcu-
55 late the force exerted between mountain ranges and their adjacent lowlands
56 that takes into account thermal structures and chemical depletion.

57

58 **2 The Variscan Foreland of the northern UK**

59 The Variscan Mountain range formed due to the collision between Gondwana
60 and Laurussia, reached its maximum intensity in the late Carboniferous, and
61 produced a Tibetan-scale orogenic belt covering central/southern Europe,
62 and parts of northern Africa and North America. The range front of the
63 northern margin of the Variscan Orogenic belt was just within the south-
64 ern UK (Figure 1). Immediately south of this line, the Variscan Orogeny
65 involved folding, cleavage formation, and low-grade metamorphism of sedi-
66 mentary rocks (e.g. Woodcock and Strachan, 2012, and references therein).
67 The metamorphic grade increases southwards into northern France, and late-
68 orogenic granites are common. Flexural foreland basin deposits are exposed
69 in some locations, immediately to the north of the Variscan front (shown in
70 blue on Figure 1). North of this flexural basin, many compressional struc-
71 tures were active in the foreland of the mountain range (e.g. Corfield et al.,
72 1996; Warr, 2012). These faults and folds, most of which reactivate pre-
73 existing features, commonly underwent displacements of hundreds of metres
74 to 1–2 km (e.g. Corfield et al., 1996; Woodcock and Rickards, 2003; Warr,
75 2012; Thomas and Woodcock, 2015). The deformation is analogous to the
76 shortening observed in the forelands of modern orogenic belts, which occurs

77 in response to the compressive force exerted between the mountains and the
78 adjacent lowlands (e.g. in the Himalayan foreland of India (e.g. Copley et al.,
79 2011) and the Andean foreland of South America (e.g. Assumpcao, 1992)).
80 In this paper we estimate an upper bound on the shear stresses required to
81 make faults slip in the Variscan foreland, by resolving the total force ex-
82 erted between the mountains and the lowlands onto the seismogenic layer
83 in the region. This estimate is an upper bound for the stresses that were
84 required to cause fault slip, because some of the total force could have been
85 supported by the ductile lithosphere. Our calculations lead to insights into
86 fault strength in addition to what has so far been achieved in the equivalent
87 modern settings because of the detailed geological mapping that has been
88 undertaken in the northern UK, which allows the geometry of the structures
89 to be estimated.

90

91 **3 Scaling between seismogenic thickness and** 92 **extensional basin width**

93 In order to estimate the seismogenic thickness during the late Carboniferous
94 in the northern UK it is necessary to construct a method to infer this value
95 from present-day observables. Previous studies have documented that the
96 maximum widths of extensional basins bounded by normal faults are related
97 to the depth extent of the faults (i.e. the seismogenic thickness) (e.g. Jack-
98 son and White, 1989; Scholz and Contreras, 1998). Deeper faults result in
99 wider basins at the surface. Establishing the modern-day scaling between
100 basin width and seismogenic thickness therefore provides a means to esti-
101 mate the seismogenic thickness in ancient deformation belts in which basin
102 widths can be observed or inferred. Figure 2 shows the relationship between
103 maximum basin width and seismogenic thickness in modern-day extensional
104 regions. The relationship between basin width and seismogenic thickness is
105 clearly visible. The boxes encompass the range of maximum basin widths
106 and seismogenic thicknesses for the fault systems in each region, estimated
107 from published mapping, tectonic geomorphology, and local and teleseismic
108 earthquake-source inversions (references given in the figure caption). We

109 only use well-constrained earthquake depths, derived from the modelling of
110 body-waveforms or recordings on dense local networks. The basin width is
111 defined using the subsidence pattern resulting from motion on the presently-
112 active basin-controlling fault (i.e. towards which the sediments in the basin
113 interior dip). Older, inactive faults on the basin margins are not included in
114 the measurements of basin width. As such, each measurement represents the
115 width of basins produced by single, major, faults, and these may be embed-
116 ded within a region that has experienced prior extension on older faults, or
117 be currently also undergoing extension on other, spatially separated, struc-
118 tures.

119

120 Extensional basins formed in the early/mid Carboniferous, which pre-
121 date the Variscan shortening in the northern UK, and are thought to repre-
122 sent back-arc extension before continent-continent collision, (e.g. Woodcock
123 and Strachan, 2012). Post-Variscan extensional basins formed in the Per-
124 mian and Triassic are thought to be related to post-orogenic collapse and
125 intra-Pangaea rifting (e.g. Woodcock and Strachan, 2012). These pre- and
126 post-Variscan basins show maximum widths of 20–30 km (e.g. the Carbonif-
127 erous Northumberland Trough, Bowland and North Staffordshire Basins, and

128 southern North Sea, and the Permian and Triassic North Minch and North
129 Lewis Basins and Worcester Graben (Stein and Blundell, 1990; Chadwick
130 et al., 1995; Corfield et al., 1996; Aitkenhead et al., 2002; Waters and Davies,
131 2006); labelled on figure 1). Although some sub-basins show smaller widths,
132 modern-day analogues demonstrate that it is the maximum basin widths in
133 a region that scale with the seismogenic thickness (as plotted on Figure 2).
134 Basin widths of 20–30 km imply a seismogenic thickness of 15–40 km in the
135 Carboniferous in the UK, based upon Figure 2. This value is similar to the
136 modern-day value of 20–25 km, based upon the well-constrained depths of
137 recent earthquakes (Baptie, 2010).

138

139 **4 The forces exerted between mountain ranges** 140 **and lowlands**

141 It has been previously described how the force exerted between an isostatically-
142 compensated mountain range and the adjacent lowlands can be calculated by
143 summing the lateral differences in the vertical normal stress between the two
144 lithospheric columns (e.g. Artyushkov, 1973; Dalmayrac and Molnar, 1981).

145 It is important to consider density differences resulting from both the thermal
146 structure of the lithosphere and also chemical depletion (e.g. England and
147 Houseman, 1989; Molnar et al., 1993). We have built upon this prior work
148 by calculating the force exerted between a mountain range and an adjacent
149 lowland using a wide range of plausible parameters, in order to estimate the
150 range of possible force magnitudes.

151

152 In our calculations we enforce isostatic compensation at the base of the
153 lithosphere, and assume that lithosphere thickness contrasts occur in pro-
154 portion to crustal thickness contrasts (as has recently shown to be the case
155 in present-day Asia; M^cKenzie and Priestley (2016)). We vary the crustal
156 thickness in the mountains from 55 to 80 km (the values of all the parameters
157 used in our calculations are given in Table 1). The density reduction caused
158 by the chemical depletion of the lithosphere relative to the asthenosphere is
159 taken to be 60 kg/m^3 , based upon geochemical results from Tibet and Iran
160 (M^cKenzie and Priestley, 2016). The crustal thickness in the lowlands has
161 been varied from 32–36 km, based on receiver functions and seismic experi-
162 ments in the UK (Davis et al., 2012). We take the lithosphere thickness in
163 the lowlands to be 120 km (M^cKenzie and Priestley, 2016). We have used

164 densities for the crust and lithospheric mantle at the Earth's surface of 2800
165 and 3330 kg/m³, have used a thermal expansion coefficient of 3×10^{-5} for
166 the crust, and the expressions of Bouhifid et al. (1996) for the temperature-
167 dependence of density in the mantle (assumed to be dominated by olivine).
168 In the lowlands we assume that the geotherm is in steady-state, which we
169 approximate as linear gradients in the crust and mantle. The temperature
170 at the base of the lithosphere is enforced to be the isentropic temperature
171 at that depth (calculated for a mantle potential temperature of 1315°). We
172 have varied the temperature of the Moho in the lowlands between 600°C and
173 700°C, which spans the range commonly suggested for regions with a simi-
174 lar crust and lithosphere thickness to the UK (e.g. Emmerson et al., 2006;
175 Copley et al., 2009). In the mountains we use the shape of the geotherms
176 calculated for southern Tibet by Craig et al. (2012), which take into account
177 the advection of heat caused by underthrusting on the margins of mountain
178 ranges. We scale these geotherms to match the thickness of the crust in the
179 mountains, and to vary the temperature at the Moho between 600°C and
180 800°C (which encompasses inferences from modern-day orogenic belts, based
181 upon thermal models and the distribution of lower-crustal earthquakes (e.g.
182 Craig et al., 2012)).

183

184 We have computed the magnitude of the force exerted between the moun-
185 tains and the lowlands for all combinations of these parameter ranges. Fig-
186 ure 3 shows the number of models that predict each value of the force, as a
187 function of the crustal thickness in the mountains. The thick dashed black
188 line shows the values obtained by assuming isostatic compensation at the
189 base of the crust, and constant densities for the crust and mantle, which
190 over-estimates the magnitude of the force. Support for our calculations is
191 provided by the independent estimates of the crustal thickness in Tibet (75–
192 80 km, e.g. Mitra et al., 2005), and the force exerted between India and Tibet
193 ($5.5 \pm 1.5 \times 10^{12}$ N/m; Copley et al., 2010), which is in the range predicted by
194 our calculations (Figure 3). Pressure-temperature estimates from high-grade
195 crustal metamorphic rocks from central Europe imply that the crust in the
196 Variscan mountains was 65–73 km thick (e.g. Kroner and Romer, 2013, and
197 references therein), so Figure 3 suggests that the force exerted between these
198 mountains and their foreland in the northern UK was $1\text{--}6 \times 10^{12}$ N per metre
199 along-strike. The inset on Figure 3 shows the relative likelihood of each force
200 value, based upon how many of the combinations of the adjustable parame-
201 ters result in each estimated value.

203 **5 Fault strength**

204 We can estimate an upper bound on the shear stresses that caused the faults
205 in the Variscan foreland to slip, by assuming that all of the force estimated
206 above is supported by the seismogenic layer. Detailed mapping of the late
207 Carboniferous shortening suggests that the motion was accommodated on
208 structures striking between 45° and 90° from the maximum compression di-
209 rection (e.g. Corfield et al., 1996; Woodcock and Rickards, 2003; Warr, 2012).
210 In common with modern-day thrusts from regions of reactivated normal-
211 faulting, and mapping of Variscan-age faults in our region of interest, we
212 vary the dip of the faults over the range $45\text{--}70^\circ$ (e.g. Sibson and Xie, 1998;
213 Woodcock and Rickards, 2003). We have conducted calculations to resolve
214 the total force exerted between the mountains and the lowlands onto the
215 foreland faults, using the method of Lamb (2006). This method balances the
216 forces exerted on the wedge of material overlying a fault, and includes both
217 the tectonic stresses and gravity acting on the mass of the rock. Because the
218 seismogenic thickness we estimate is smaller than, or similar to, the crustal

219 thickness, we use only a single fault rheology (rather than using different pa-
220 rameters to represent the crustal and mantle, as done by Lamb (2006)). We
221 use the range of fault strikes and dips described above, along with the range
222 of possible seismogenic thickness estimated above, and the distribution of es-
223 timated forces shown in the inset on Figure 3. Our results for the maximum
224 shear stresses supported by the faults are shown in Figure 4. The maximum
225 shear stress is most likely to be in the range 10–100 MPa (which encom-
226 passes 90% of the models), with a nominal most likely value of 37.5 MPa.
227 The corresponding upper bound on the effective coefficient of friction when
228 these faults slipped is most likely to be in the range 0.02–0.24 (which encom-
229 passes 90% of the models), with a nominal most likely value of 0.08. This
230 range is considerably lower than predicted by ‘Byerlee’s Law’ (i.e. 0.6–0.8).
231 For the faults to have slipped in response to the calculated force implies
232 intrinsically weak fault rocks in the reactivated fault zones, high pore fluid
233 pressures, or both. If some of the force transmitted through the Variscan
234 foreland was supported by stresses in the ductile lithosphere, then the faults
235 would be weaker than estimated here. In addition, the above analysis im-
236 plicitly assumes that the deviatoric stresses in the Variscan Mountains are
237 minor, and that the majority of the force calculated above is supported by

238 the lithosphere in the foreland of the range. However, if significant stresses
239 are supported elsewhere, e.g. by driving the viscous flow of the mountains
240 over the underthrusting foreland, then the faults would be weaker than our
241 estimate.

242

243 A striking feature of the late Carboniferous shortening in the northern
244 UK is that many structures were active at an oblique angle to the maximum
245 shortening direction (Figure 1). The faults that have been studied in detail
246 (e.g. the Dent Fault; Woodcock and Rickards (2003); Thomas and Wood-
247 cock (2015); labelled on Figure 1) were pre-existing structures that were
248 re-activated in the late Carboniferous. Fault motion at an oblique angle is
249 less energetically-favourable than motion on an optimally-oriented fault (i.e.
250 perpendicular to the shortening direction, and with a dip that is optimum
251 for the coefficient of friction). We can estimate how much weaker these pre-
252 existing faults must be than optimally oriented, but un-faulted, planes by
253 resolving forces in these two configurations. Specifically, we resolve the total
254 force estimated above onto planes with the dips and orientations observed in
255 the northern UK, and onto faults that strike perpendicular to the maximum
256 principal stress and dip at angles optimum for their coefficient of friction.

257 The differences in resolved stresses in these two geometries allow us to in-
258 fer how much weaker pre-existing faults must be than intact rock, in order
259 for reactivation to have occurred, rather than the formation of new faults.
260 We find that the re-activated structures must have an effective coefficient of
261 friction at least 30% lower than intact rock in order for them to have been
262 reactivated, rather than new faults initiating.

263

264 **6 Conclusions**

265 We have described how to estimate the seismogenic thickness in ancient de-
266 formation belts, and have estimated the forces exerted between mountain
267 ranges and lowlands by including thermal and chemical effects on the den-
268 sity. Combining these results for the deformation in the foreland of the
269 Variscan Mountains in the northern UK shows that the faults had a low ef-
270 fective coefficient of friction (i.e. 0.02–0.24), and were at least 30% weaker
271 than un-faulted rock.

272

273 **7 Acknowledgements**

274 We thank Simon Lamb and one anonymous reviewer for helpful comments on
275 the manuscript, and the participants in the 2015 Cambridge Earth Sciences
276 field trip to Sedbergh for stimulating discussions. This work forms part of
277 the NERC- and ESRC-funded project ‘Earthquakes without Frontiers’, and
278 was partially supported by the NERC grant ‘Looking Inside the Continents
279 from Space’.

280

References

- N. Aitkenhead, W.J. Barclay, A. Brandon, R.A. Chadwick, M.J.I. Chisholm, A.H. Cooper, and E.W. Johnson. *British Regional Geology: the Pennines and adjacent areas (4th edition)*. HMSO, London, 2002.
- B.P. Allmann and P.M. Shearer. Global variations of stress drop for moderate to large earthquakes. *J. Geophys. Res.*, 114:doi:10.1029/2008JB005821, 2009.
- E.V. Artyushkov. Stresses in the lithosphere caused by crustal thickness inhomogeneities. *J. Geophys. Res.*, 78:7675–7708, 1973.
- M. Assumpcao. The regional intraplate stress field in South America. *J. Geophys. Res.*, 97:11,889–11,903, 1992.
- B. Baptie. Seismogenesis and state of stress in the UK. *Tectonophysics*, 482: 150–159, 2010.

- K-P. Bonjer. Seismicity pattern and style of seismic faulting at the eastern borderfault of the southern Rhine Graben. *Tectonophysics*, 275:41–69, 1997.
- M.A. Bouhifid, D. Ardault, G. Fiquet, and P. Richet. Thermal expansion of forsterite up to the melting point. *Geophys. Res. Lett.*, pages 1143–1146, 1996.
- British Geological Survey. Tectonic map of Britain, Ireland and adjacent areas, 1996. British Geological Survey, Nottingham.
- M. Brudy, M.D. Zoback, K. Fuchs, F. Rummel, and J. Baumgartner. Estimation of the complete stress tensor to 8 km depth in the KTB scientific drill holes: Implications for crustal strength. *J. Geophys. Res.*, 102:18,453–18,475, 1997.
- J. Byerlee. Friction of rocks. *Pure. Appl. Geophys.*, 116:615–626, 1978.
- R.A. Chadwick, D.W. Holliday, S. Holloway, and A.G. Hulbert. The structure and evolution of the Northumberland-Solway Basin and adjacent areas. British Geological Survey Subsurface Memoir, HMSO, London, 1995.
- B. Cheng, S. Cheng, G. Zhang, and D. Zhao. Seismic structure of the Helan-LiupanOrdos western margin tectonic belt in north-central China and its geodynamic implications. *Journal of Asian Earth Sciences*, 87:141–156, 2014.
- C. Collettini and R.H. Sibson. Normal faults, normal friction? *Geology*, 29:927–930, 2001.
- A. Copley, F. Boait, J. Hollingsworth, J. Jackson, and D. McKenzie. Sub-parallel thrust and normal faulting in Albania and the role of gravitational potential energy and rheology contrasts in mountain belts. *J. Geophys. Res.*, 114:doi:10.1029/2008JB005931, 2009.
- A. Copley, J-P. Avouac, and J-Y. Royer. The India-Asia collision and the Cenozoic slowdown of the Indian plate: implications for the forces driving plate motions. *J. Geophys. Res.*, 115:doi:10.1029/2009JB006634, 2010.
- A. Copley, J-P. Avouac, J. Hollingsworth, and S. Leprince. The 2001 Mw 7.6 Bhuj earthquake, low fault friction, and the crustal support of plate

- driving forces in India. *J. Geophys. Res.*, 116:doi:10.1029/2010JB008137, 2011.
- S.M. Corfield, R.L. Gawthorpe, M. Gage, A.J. Fraser, and B.M. Besley. Inversion tectonics of the Variscan foreland of the British Isles. *Journal of the Geological Society*, 153:17–32, 1996.
- T. Craig, A. Copley, and J. Jackson. Thermal and tectonic consequences of india underthrusting tibet. *Earth Planet. Sci. Lett.*, 353–354:231–239, 2012.
- T. Craig, A. Copley, and T. Middleton. Constraining fault friction in oceanic lithosphere using the dip angles of newly-formed faults at outer rises. *Earth Planet. Sci. Lett.*, 392:94–99, 2014.
- T.J. Craig, J.A. Jackson, K. Priestley, and D. McKenzie. Earthquake distribution patterns in Africa: their relationship to variations in lithospheric and geological structure, and their rheological implications. *Geophys. J. Int.*, 185:403–434, 2011.
- B. Dalmayrac and P. Molnar. Parallel thrust and normal faulting in Peru and constraints on the state of stress. *Earth Planet. Sci. Lett.*, 55:473–481, 1981.
- M.W. Davis, N.J. White, K.F. Priestley, B.J. Baptie, and F.J. Tilmann. Crustal structure of the British Isles and its epeirogenic consequences. *Geophys. J. Int.*, 190:705–725, 2012.
- B. Emmerson, J. Jackson, D. McKenzie, and K. Priestley. Seismicity, structure, and rheology of the lithosphere in the Lake Baikal region. *Geophys. J. Int.*, 167:1233–1272, 2006.
- P. England and G. Houseman. Extension during continental convergence, with application to the Tibetan plateau. *J. Geophys. Res.*, 94:17561–17579, 1989.
- D. Hatzfeld, A.A. Christodoulou, E.M. Scordilis, D. Panagiotopoulos, and P.M. Hatzidimitriou. A microearthquake study of the Mygdonian graben (northern Greece). *Earth Planet. Sci. Lett.*, 81:379–396, 1987.

- D. Hatzfeld, V. Karakostas, M. Ziazia, I. Kassaras, E. Papadimitriou, K. Makropoulos, N. Voulgaris, and C. Papaioannou. Microseismicity and faulting geometry in the Gulf of Corinth (Greece). *Geophys. J. Int.*, 141: 438–456, 2000.
- G.A. Ichinose, J.G. Anderson, K.G. Smith, and Y. Zeng. Source parameters of Eastern California and Western Nevada earthquakes from regional moment tensor inversion. *Bull. Seismol. Soc. Am.*, 93:61–84, 2003.
- J. A. Jackson and N. J. White. Normal faulting in the upper continental crust: Observations from regions of active extension. *J. Struct. Geol.*, 11: 15–36, 1989.
- E. Jacques, J.C. Ruegg, J.C. Lepine, P. Tapponnier, G.C.P. King, and A. Omar. Relocation of $M > 2$ events of the 1989 Dobi seismic sequence in Afar: evidence for earthquake migration. *Geophys. J. Int.*, 138:447–469, 1999.
- H. Kanamori and D.L. Anderson. Theoretical basis of some empirical relations in seismology. *Bull. Seismol. Soc. Am.*, 65:1073–1095, 1975.
- U. Kroner and R.L. Romer. Two plates - many subduction zones: The Variscan orogeny reconsidered. *Gondwana Research*, 24:298–329, 2013.
- S. Lamb. Shear stresses on megathrusts: Implications for mountain building behind subduction zones. *J. Geophys. Res.*, 111: doi:10.1029/2005JB003916, 2006.
- X. Liang, S. Zhou, Y.J. Chen, G. Jin, L. Xiao, P. Liu, Y. Fu, Y. Tang, X. Lou, and J. Ning. Earthquake distribution in southern Tibet and its tectonic implications. *J. Geophys. Res.*, 113:doi:10.1029/2007JB005101, 2008.
- D.A. Lockner, C. Morrow, D. Moore, and S. Hickman. Low strength of deep San Andreas fault gouge from SAFOD core. *Nature*, 472:82–85, 2011.
- D. McKenzie and K. Priestley. Speculations on the formation of cratons and cratonic basins. *Earth Planet. Sci. Lett.*, 435:94–104, 2016.
- T.A. Middleton and A. Copley. Constraining fault friction by re-examining earthquake nodal plane dips. *Geophys. J. Int.*, 196:671–680, 2014.

- S. Mitra, K. Priestley, A.K. Bhattacharyya, and V.K. Gaur. Crustal structure and earthquake focal depths beneath northeastern India and southern Tibet. *Geophys. J. Int.*, 160:227–248, 2005.
- P. Molnar, P. England, and J. Martinod. Mantle dynamics, uplift of the Tibetan plateau, and the Indian monsoon. *Reviews of Geophysics*, 31: 357–396, 1993.
- W.D. Richins, J.C. Pechmann, R.B. Smith, C.J. Langer, S.K. Goter, J.E. Zollweg, and J.J. King. The 1983 Borah Peak, Idaho, earthquake and its aftershocks. *Bull. Seismol. Soc. Am.*, 77:694–723, 1987.
- A. Rigo, H. Lyon-Caen, R. Armijo, A. Deschamps, D. Hatzfeld, K. Makropoulos, P. Papadimitriou, and I. Kassaras. A microseismic study in the Gulf of Corinth (Greece): Implications for large-scale normal faulting mechanisms. *Geophys. J. Int.*, 126:663–688, 1996.
- C. H. Scholz and J. C. Contreras. Mechanics of continental rift architecture. *Geology*, 26:967–970, 1998.
- R.H. Sibson and G. Xie. Dip range for intracontinental reverse fault ruptures: Truth not stranger than friction? *Bull. Seismol. Soc. Am.*, 88:1014–1022, 1998.
- A.M. Stein and D.J. Blundell. Geological inheritance and crustal dynamics of the northwest Scottish continental shelf. *Tectonophysics*, 173:455–467, 1990.
- C.W. Thomas and N.H. Woodcock. The kinematic linkage of the Dent, Craven, and related faults of Northern England. *Proceedings of the Yorkshire Geological Society*, 60:258–274, 2015.
- J. Townend and M.D. Zoback. How faulting keeps the crust strong. *Geology*, 28:399–402, 2000.
- K. Ujiie, H. Tanaka, T. Saito, A. Tsutsumi, J.J. Mori, J. Kameda, E.E. Brodsky, F.M. Chester, N. Eguchi, S. Toczko, Expedition 343, and 343T Scientists. Low coseismic shear stress on the Tohoku-Oki megathrust determined from laboratory experiments. *Science*, 342:1211–1214, 2013.

- K. Vanneste, T. Camelbeeck, and K. Verbeek. A model of composite seismic sources for the Lower Rhine Graben, northwest Europe. *Bull. Seismol. Soc. Amer.*, 103:984–1007, 2013.
- L.N. Warr. The Varican orogeny: the welding of Pangaea. In N. Woodcock and R. Strachan, editors, *Geological history of Britain and Ireland*. Wiley-Blackwell, 2012.
- C.N. Waters and S.J. Davies. Carboniferous: extensional basins, advancing deltas and coal swamps. In P.J. Brenchley and P.F. Rawson, editors, *The geology of England and Wales, 2nd edition*. The Geological Society, London, 2006.
- N. Woodcock and R. Strachan. *Geological history of Britain and Ireland*. Wiley-Blackwell, 2012.
- N.H. Woodcock and B. Rickards. Transpressive duplex and flower structure: Dent fault system, NW England. *Journal of Structural Geology*, 25:1981–1992, 2003.

Adjusted parameters:		
Parameter	minimum value	maximum value
Seismogenic thickness in lowlands (km)	15	40
Crustal thickness in mountains (km)	55	80
Crustal thickness in lowlands (km)	32	36
Moho temperature in mountains ($^{\circ}\text{C}$)	600	800
Moho temperature in lowlands ($^{\circ}\text{C}$)	600	700
Fault strike w.r.t. max. principal stress	45°	90°
Foreland fault dips	45°	70°

Fixed parameters:	
Parameter	Value
Density difference from depletion (kg/m^3)	-60
Lithosphere thickness in lowlands (km)	120
Crust density at 0°C (kg/m^3)	2800
Lithospheric mantle density at 0°C (kg/m^3)	3330
Thermal expansion co-eff of crust	3×10^{-5}
Thermal expansion in mantle	Bouhifid et al. (1996)
Mantle potential temperature	1315°C

Table 1: Parameters used in the calculations.

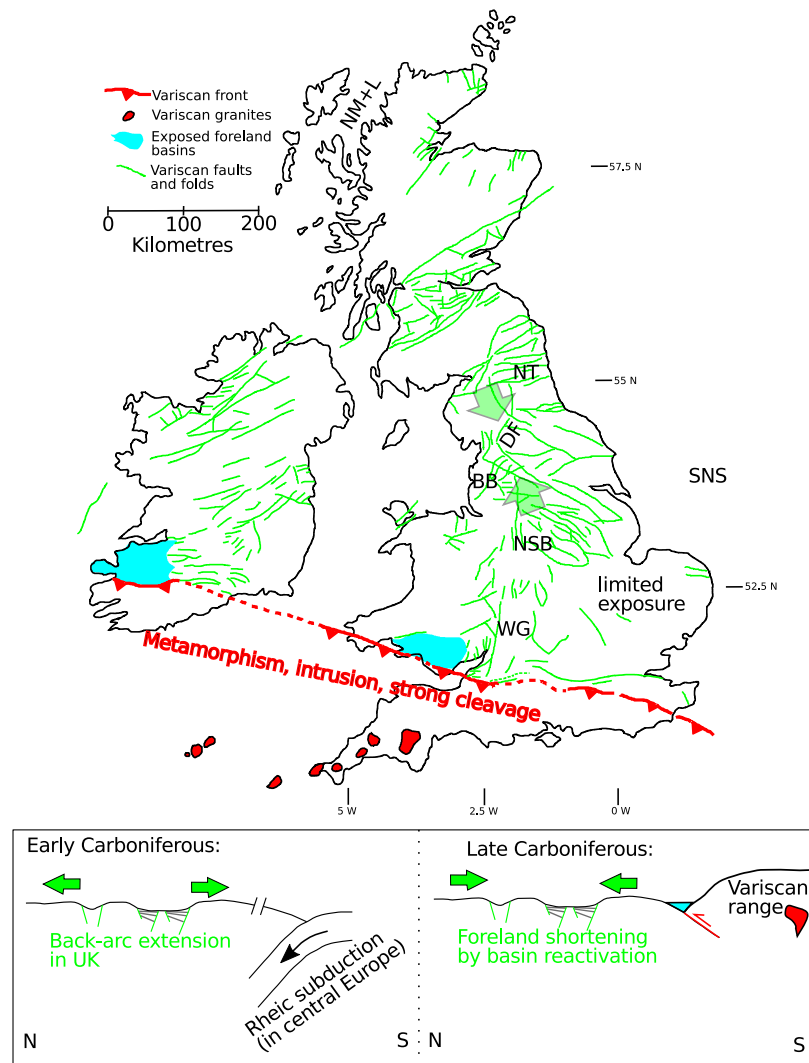


Figure 1: Summary of Variscan tectonics of the UK, adapted from Warr (2012), after British Geological Survey (1996). Metamorphism and intrusion occurred in the region to the south of the red line, which marks the Variscan range-front. Blue shading shows exposed areas of the Variscan foreland basin. Green lines show faults and folds that were active in the foreland of the Variscan mountain range. The green arrows in the centre of the map show the regional shortening direction estimated by Woodcock and Rickards (2003). DF denotes the Dent Fault. Other black labels show the locations of Carboniferous and Permian-Triassic extensional basins mentioned in the text. NM+L: North Minch and North Lewis Basins; NT: Northumberland Trough; BB: Bowland Basin; NSB: North Staffordshire Basin; WG: Worcester Graben; SNS: Southern North Sea.²⁴ The lower diagrams show schematic cross-sections during early and late carboniferous times.

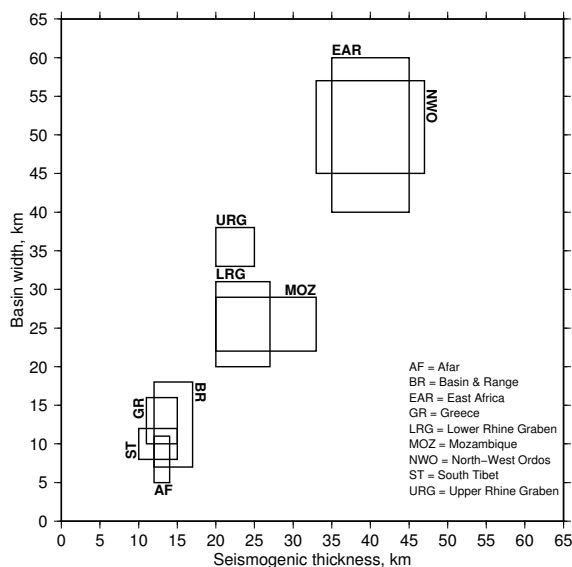


Figure 2: Relationship between the seismogenic thickness and maximum basin width for regions undergoing present-day extension. Each box represents earthquakes and basins in a different region, described in detail below. The specific areas were selected based on the availability of multiple earthquakes with well-constrained depths that clearly delimit the seismogenic thickness, and clearly-defined extensional basins. GR: the gulfs of Corinth and Evia, and Thessaloniki, Greece (Hatzfeld et al., 1987; Rigo et al., 1996; Hatzfeld et al., 2000); AF: Dobi graben, central Afar (Jacques et al., 1999); ST: central southern Tibet (Liang et al., 2008); BR: Borah Peak region, plus eastern California and western Nevada, Basin and Range, USA (Richins et al., 1987; Ichinose et al., 2003); LRG: Lower Rhine Graben (Vanneste et al., 2013); URG: Upper Rhine Graben (Bonjer, 1997); MOZ: Mozambique (Craig et al., 2011); EAR: western branch of the East African Rift (Craig et al., 2011, and references therein); NWO: north-west margin of Ordos (Cheng et al., 2014).

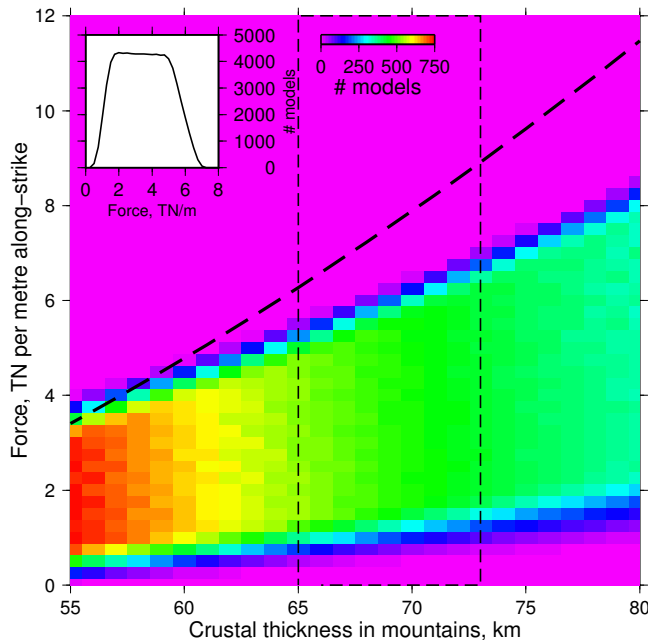


Figure 3: Distribution of forces exerted between an isostatically-compensated mountain range and the adjacent lowlands, calculated using the range of parameters described in the text. The main figure shows the number of models that predict each value of the force, as a function of the crustal thickness in the mountains. The inset shows the distribution of model results for all values of the crustal thickness in the mountains from 65 to 73 km, marked by the thin dashed lines on the main Figure. The thick dashed line shows the force calculated assuming isostatic compensation at the base of the crust and constant densities of 2800 and 3300 kg/m³ for the crust and mantle.

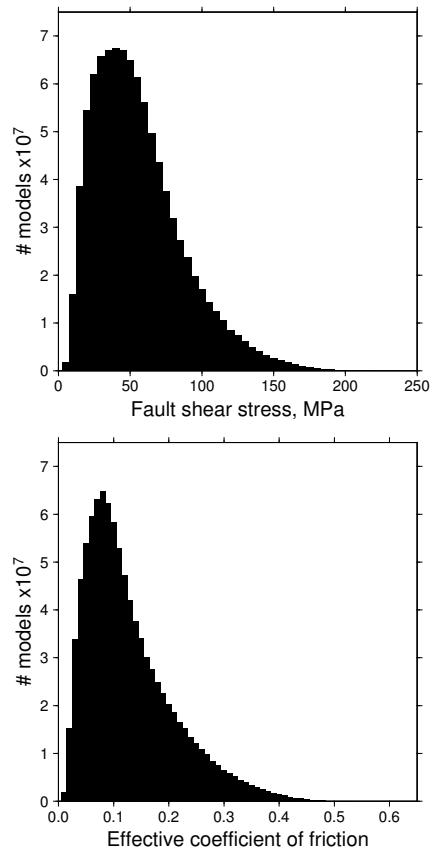


Figure 4: Estimates of the maximum possible fault shear stress (top) and effective coefficient of friction (bottom) in the Variscan foreland of the northern UK, based on the ranges of parameters described in the text.